Highlighting properties of filters for their application in temporal phase shifting interferometry

Vanessa Rosso[a*], Fabrice Michel[b], Vincent Moreau[b], Yvon Renotte[a], Bernard Tilkens[b], Yves Lion[a]

[a]HOLOLAB, Department of Physics, Bat. B5a, Université de Liège, B-4000 Liège, Belgium
[b]DEIOS s.a., Liège Science Park - Spatiopole, rue des Chasseurs Ardennais (WSL), B-4031 Angleur, Belgium

ABSTRACT

The goal of this work is to develop a simple and systematic method to highlight the properties of filters for their application in temporal phase shifting interferometry. In this study, the effects of elementary filters (mean, gaussian and median masks) are analyzed. In order to compare those filters, correlation fringes were numerically synthesized and a Gaussian noise has been added. The advantages and the failures of each studied filtering mask have been enhanced thanks to the comparison of different profiles and fidelity functions. Finally, this study is applied to the filtering of a shearogram recorded in our laboratory.

Keywords: noise filtering, temporal phase shifting interferometry, shearogram

1. INTRODUCTION

In the last few years, temporal phase shifting interferometry (digital speckle pattern interferometry[1], digital shearography[2], fringes projection[3],…) has emerged as a new efficient technique for metrological applications (e.g. three dimensional shape measurement, surface displacements or strains…[1-3]). Those interferometric techniques yield a wrapped phase map. In order to obtain quantitative measurements, a complete elimination of noise in the wrapped phase map is an essential precondition. Moreover only a fringe pattern undisturbed by phase filtering guarantees successful use of the phase unwrapping method[2, 4].

Some researchers working on temporal phase shifting interferometry develop their own masks or transforms for filtering the phase map while others prefer using commercial softwares as an easier solution. The goal of this work is to develop a simple and systematic method to highlight the properties of filters in order to be easily transposed to the study of more complex filters and, consequently, encouraging researchers to create and study their own filtering software.

In this work the effects of classical and elementary filters (mean, Gaussian and median masks) are analyzed. In order to compare those filters, correlation fringes were numerically synthesized. Gaussian noise has been added to these fringes with the aim of obtaining fringes similar to the ones obtained experimentally in speckle interferometry, i.e. the experimental technique for which filtering is essential.
In order to compare objectively the filtered simulated fringes with the noiseless ones, different profiles showing the irradiance along the abscissa axis X for a fixed value of the ordinate Y have been extracted and then superimposed. A fidelity function has also been defined, it permits to quantify the correspondence between the noiseless simulated fringes and the ones obtained after filtering. The advantages and the failures of each studied filtering mask have thus been enhanced. Finally, this study is applied to the filtering of a shearogram recorded in our laboratory.

* Vanessa.Rosso@ulg.ac.be; phone +32 4 3663627 ; fax +32 4 3664516

Photonic Applications in Biosensing and Imaging, edited by Warren C. W. Chan, Kui Yu, Ulrich J. Krull, Richard I. Hornsey, Brian C. Wilson, Robert A. Weersink, Proc. of SPIE Vol. 5969, 59692M, (2005) · 0277-786X/05/$15 · doi: 10.1117/12.629913

2. THEORY

2.1. Filtering by mean, Gaussian and median masks

In temporal phase shifting interferometry, the wrapped phase map is generally filtered pixel by pixel thanks to the use of masks[2, 4]. The latter are usually square matrices of odd dimension *n*. The parity and dimension of the mask are justified by the essential role of the central element of the matrix.

An intuitive mask to use for filtering is the mean mask. The mask is moved around each pixel of the image and the irradiance of the considered pixel is replaced by a mean irradiance I_m depending on the value of the weighting factors and the dimension *n* of the mask. The weighting factors, or coefficients, of the mean mask are unity. If *K(i,j)* is the value of the coefficient *(i,j)* of the mask, if *g(i,j)* is the irradiance of the pixel covered by the coefficient *(i,j)* of the mask and *S*, the sum of the weighting factors *K(i,j)*, then the mean irradiance I_m of the pixel covered by the central element $\left(\frac{n+1}{2}, \frac{n+1}{2}\right)$ of the mask, is given by the relationship:

$$I_m = \frac{1}{S}\sum_{i=1}^{n}\sum_{j=1}^{n} K(i,j)g(i,j) \tag{1}$$

The mean mask has weighting factors *K(i,j)* equal to unity. In order to give more importance to the irradiance of the considered pixel, the literature[2] proposes to use weighting factors *K(i,j)* distributed following a two dimensional Gaussian law and centered on the central element of the mask. This mask is then called "Gaussian mask" and its use is similar to the mean one (see Eq. (1)).

The wrapped phase map can also be filtered easily by a median filter. Contrary to the mean and Gaussian masks, the median mask is defined from the image itself and, hence, is different for each pixel of the image to be filtered. Indeed, the coefficient *K(i,j)* of the mask is imposed to be equal to the irradiance *g(i,j)*, i.e. the irradiance of the pixel covered by the element *(i,j)* of the mask. When the mask relative to the considered pixel is built, its coefficients are sorted by ascending order in a vector. The irradiance of the central element of that sorted vector becomes the new irradiance for the analyzed pixel.

2.2. Effects of the different filtering masks

In order to highlight the advantages or failures of different filtering masks, it is possible to compare their long-term effects on a wrapped phase map obtained experimentally. However, in that case, the profile of noiseless fringes is unknown and, consequently, any conclusion about which mask is the most efficient cannot be drawn. The literature[4, 5] thus suggests synthesizing numerically a wrapped phase map as a reference and then adding a Gaussian noise. The goal of this work is to find out which mask is the most efficient with regard to the reduction of noise but without loss of information.

It is necessary to use comparison tools to enhance the differences between filtered images and the reference phase map. The first one is the simple visualization of the filtered phase map. It permits a qualitative analysis of filtering but is mainly subjective. In order to compare objectively the filtered simulated fringes with the noiseless ones, different profiles showing the irradiance along the abscissa axis X for a fixed value of the ordinate Y will be extracted and then superimposed. Finally, the filtering techniques will be compared quantitatively thanks to the fidelity function *F* of the filtered images[5], defined as follows:

$$F = 1 - \frac{\sum_{x,y}\left[I_{filt}(x,y) - I_{ref}(x,y)\right]^2}{\sum_{x,y} I_{ref}^2(x,y)} \tag{2}$$

where $I_{filt}(x,y)$ is the irradiance distribution of the considered filtered image and $I_{ref}(x,y)$, the irradiance of the noiseless simulated wrapped phase map. The sums are carried out on all the pixels of the images. In short, the fidelity function permits to quantify the correspondence between the noiseless simulated fringes and the ones obtained after filtering.

3. RESULTS AND DISCUSSION

3.1. Influence of the filtering place

Fig. 1.a and Fig. 1.b represent respectively the synthesized correlation fringes and the same ones where a Gaussian noise has been added. The simulation program was realized with the LabView® software (National Instruments). For image processing, the image is converted in a matrix. The value of the element *(x,y)* of the matrix, in grey levels, corresponds to the irradiance of the pixel *(x,y)* in the detector. The simulated images have 512 pixels x 512 pixels and 256 grey levels. Fig. 2 shows a cut of the images shown in Fig. 1.a and Fig. 1.b along the abscissa axis X for an arbitrary ordinate Y. The ordinate Y is fixed at the value 250 pixels for all the following profiles.

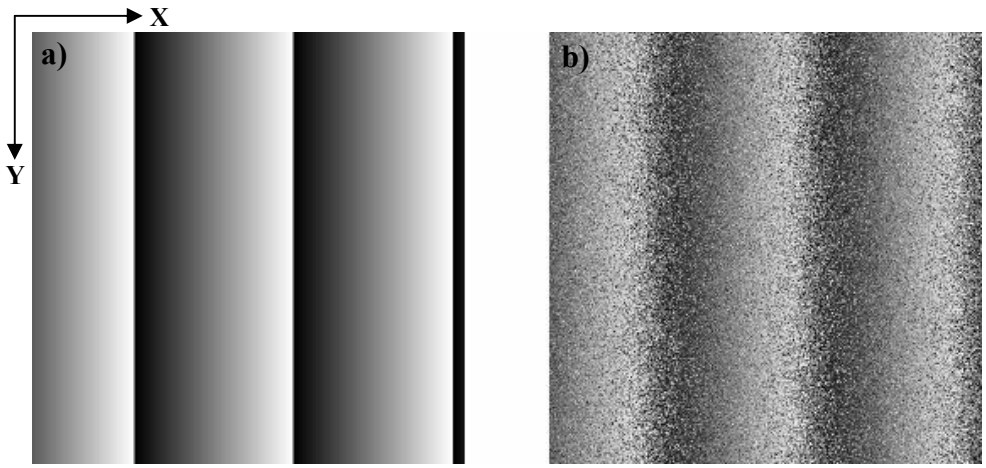

Fig. 1. a) Simulated correlation fringes (reference image) b) Correlation fringes of Fig. 1.a disturbed by a Gaussian noise.

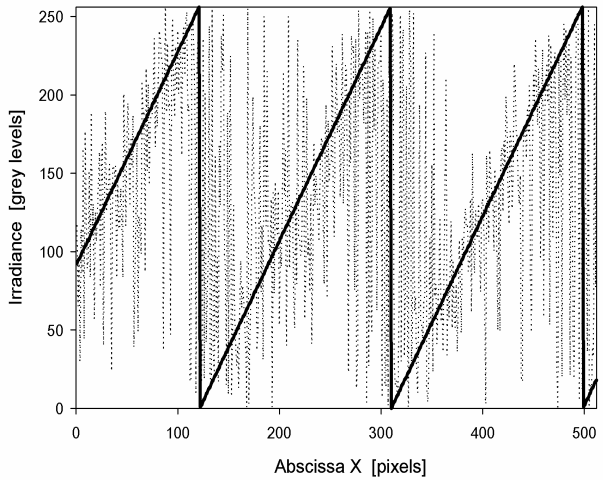

Fig. 2. Profiles of the reference fringes in Fig.1.a (continuous line) and the reference fringes disturbed by a Gaussian noise in Fig. 1.b (dotted line).

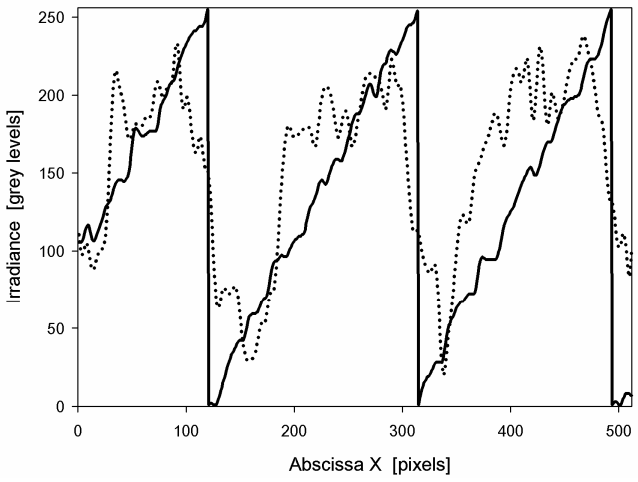

Fig. 3. Profiles of fringes filtered three times by a mean mask of dimension 5. Filtering place: phase map (dotted line), sine/cosine (continuous line).

The dotted line of Fig. 3 shows the effect of a mean mask of dimension 5 applied three times on the disturbed phase map of Fig. 1.b. This profile shows that the filtering induces an important loss of phase steps: the initial sawtooth function seems to become sinusoidal. This effect makes the phase unwrapping process hard to realize, even impossible.

In order to avoid this problem, the literature[2, 4] suggests filtering the numerator and denominator of the distribution $tan\Delta(x,y)$, where $\Delta(x,y)$ is the considered wrapped phase distribution in temporal phase shifting interferometry. Indeed, those numerator and denominator correspond respectively with sine and cosine functions, the filtering will mainly induce their smoothing. The phase steps will be rebuilt when the function arctan is applied on the filtered distribution $tan\Delta(x,y)$, this is confirmed by the continuous line in Fig. 3. In agreement with these observations, in the following the filtering will be applied on the numerator (sine) and denominator (cosine) of $tan\Delta$.

3.2. Design of a new simulated wrapped phase map

The disturbed correlation fringes simulated above yield filtered fringes similar to the reference ones and, thus, don't reveal the effects of the different masks. That is due to their profile linearity but also to their low spatial frequency. The new numerically synthesized wrapped phase map will contain a signal that will be impaired by the filtering process. The study of that disrepair will permit to highlight the qualities and defects of the different masks. In order to analyze the filter behaviour with regard to a wide range of spatial frequencies, the signal added to the first simulated fringes is chosen rectangular. Fig. 4 shows the new simulated reference correlation fringes (Fig. 4.a), the same ones disturbed with a Gaussian noise (Fig. 4.b) and the corresponding profiles (Fig. 4.c).

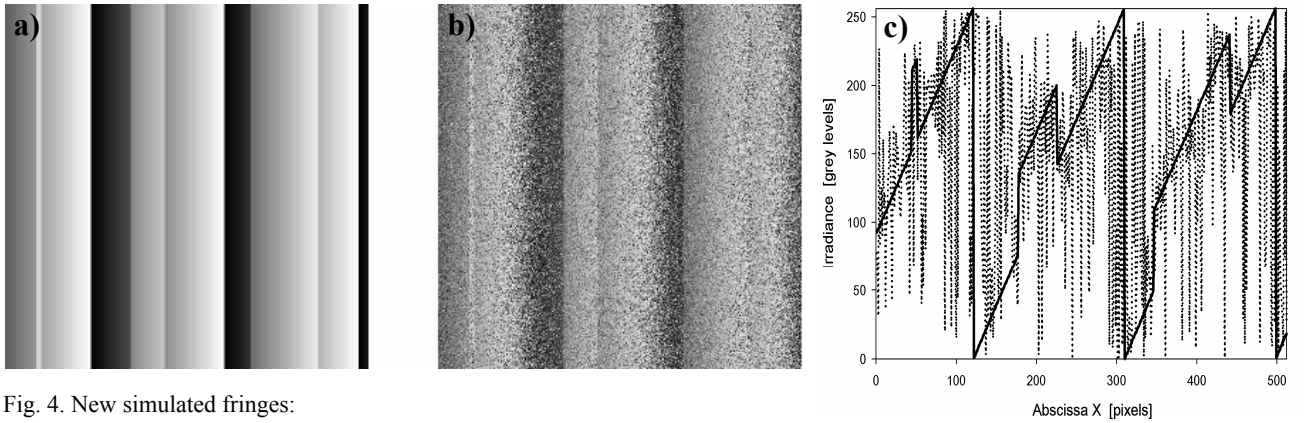

Fig. 4. New simulated fringes:

a) Reference fringes

b) Fringes of Fig. 4.a disturbed by a Gaussian noise

c) Profiles of fringes in Fig. 4.a (continuous line) and Fig. 4.b (dotted line).

3.3. Effects of the different filtering masks

3.3.1. Effect of the mean mask

Fig. 5 shows the profile of the reference wrapped phase map and the profile of the fringes filtered 40 times (a long-term effect is studied) by a mean mask of dimension 5. In this figure, it can be seen that the mean filter acts like a low-pass filter: edges of the rectangular signals are smoothed and the noise removed. Elimination of high spatial frequencies yields noiseless images but induces a loss of contrast of the signal fringes (Fig. 7.a and Fig. 7.b). A slight displacement of the phase steps is sometimes induced (Fig. 5). The mean filter behaviour is due to the average realized during the filtering process (section 2.2).

The fidelity function versus the number of filterings applied to the wrapped phase map is presented in Fig. 6 for different dimensions n of the mean mask. In the Fig. 6, it is shown that for any dimension of the mean mask, the graph of the fidelity versus the number of filterings has the same behaviour: the fidelity increases till a maximum, "the optimal fidelity F_{opt}", and then decreases. The range of increasing fidelity corresponds with the noise elimination while its decrease depicts the loss of high frequencies of the rectangular signal. The fidelity curve (Fig. 6) also teaches the higher the filter dimension, the narrower the range of the optimal fidelity. Moreover, if the filter dimension is high, then the optimal fidelity is reached for a low value of the number of filterings. On the other hand, in the studied example, for any dimension of the mean mask, the optimal fidelity reaches 97.4 %.

Finally, it is noted (see Fig.7) that when the optimal fidelity is reached, the filtered wrapped phase map are quasi-identical for any dimension of the used mean mask. As an example, the Fig. 7.a and Fig. 7.b present the wrapped phase map filtered respectively 37 times by a mean mask of dimension 3 and 4 times by a mean mask of dimension 7. The corresponding profiles are shown in Fig. 7.c.

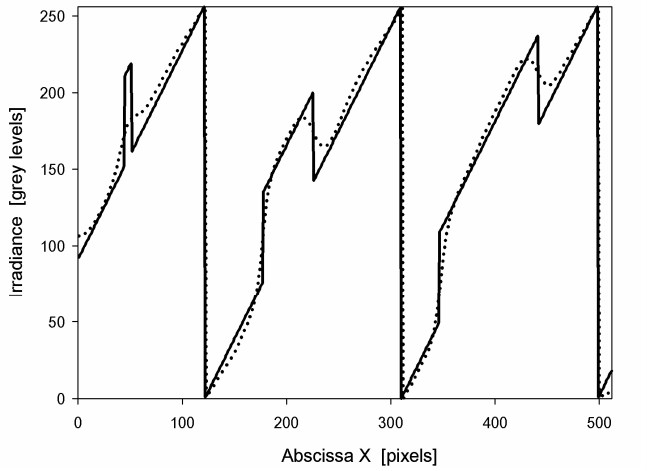

Fig. 5. Profile of the reference fringes (continuous line) and the ones filtered 40 times by a mean mask of dimension 5 (dotted line).

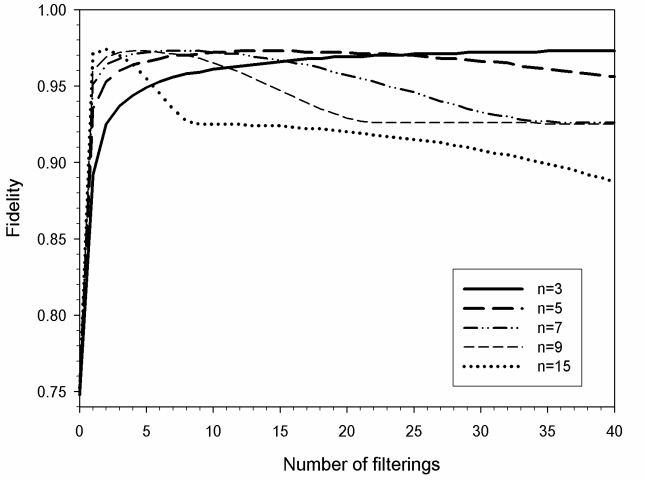

Fig. 6. Evolution of the fidelity versus the number of filterings for mean masks of dimension: 3, 5, 7, 9 and 15.

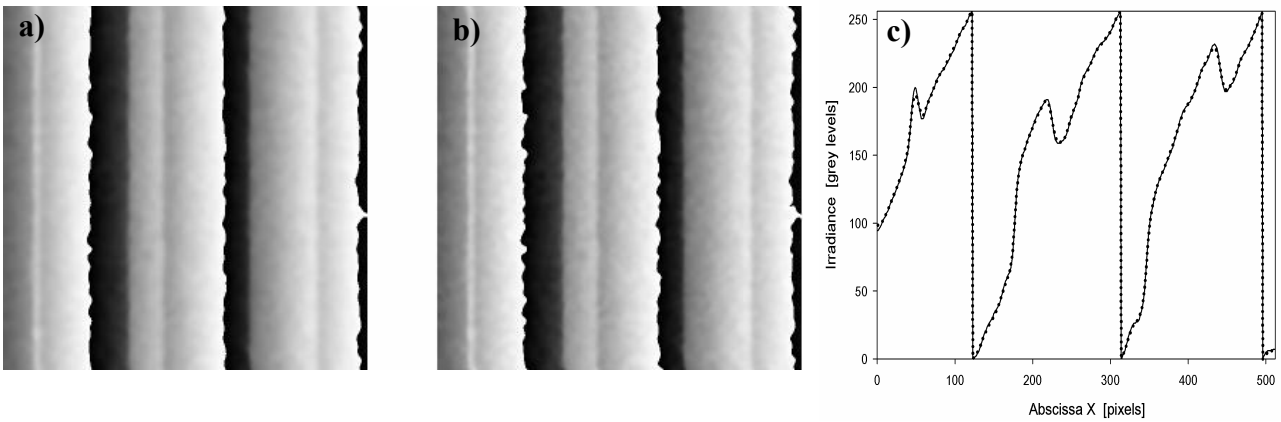

Fig. 7. Correlation fringes at the optimal fidelity F_{opt}=97.4 %.

a) Correlation fringes filtered 37 times by a mean mask of dimension 3.

b) Correlation fringes filtered 4 times by a mean mask of dimension 7.

c) Profiles of the Fig. 7.a and Fig. 7.b: they are superimposed.

3.3.2. Effect of the Gaussian mask

The profiles of reference fringes and fringes filtered 40 times by a Gaussian mask of dimension 5 and a variance σ^2=*0.1* and σ^2=*0.2 pixels*^{2} are presented in Fig. 8. It is shown in this figure that the Gaussian filter produces the same effects then the mean mask but with a more slowly elimination, in terms of the number of filterings, of the high spatial frequencies. This behaviour permits a better conservation of the rectangular signals but induces a less significant reduction of noise. The fringes filtered by a Gaussian mask are thus more contrasted but more disturbed by noise compared with the ones obtained after filtering by a mean mask.

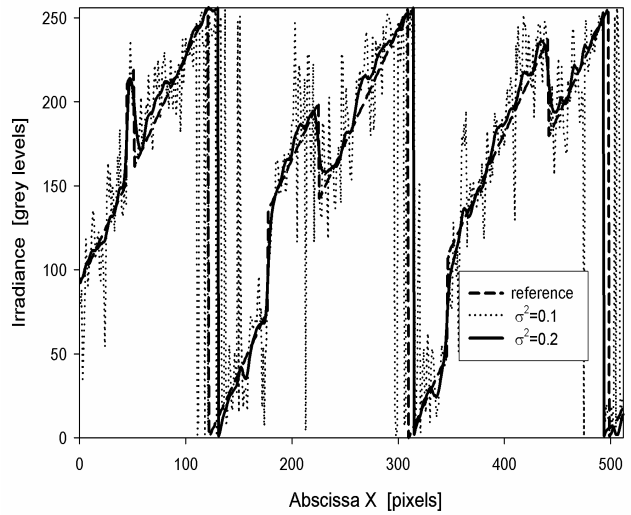

Fig. 8. Profiles of reference fringes and fringes filtered 40 times by a Gaussian mask of dimension 5 and a variance σ^2*=0.1 and 0.2 pixels*^{2}.

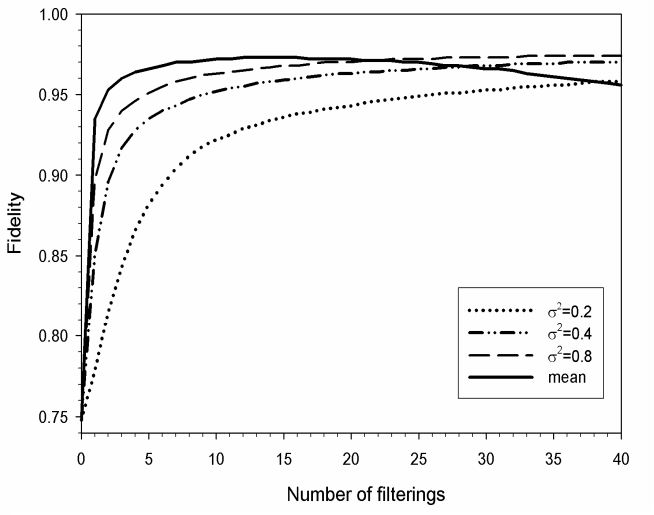

Fig. 9. Evolution of the fidelity versus the number of filterings for a mean mask of dimension 5 and Gaussian masks of dimension 5: σ^2*=0.2, 0.4 and 0.8 pixels*^{2}.

The influence of the standard deviation σ on the Gaussian mask effect has been studied and it was observed that if the variance σ^2 increases, then high frequencies are removed more quickly (see Fig. 8). Indeed, if σ^2 has a high value, then the weight of the central element of the mask will be similar to the other *K(i,j)* coefficients (see Eq. (1)) and, hence, the Gaussian filter will converge towards a mean filter of the same dimension. Consequently, in order to use the Gaussian filter for its own properties and not for the properties of the mean filter, it is recommended to use the Gaussian mask with a low variance (e.g. σ^2*=0.2 pixels*^{2}).

The low speed of high frequencies elimination drives to a fidelity that increases more slowly then the one obtained with the mean mask, as it is shown in Fig. 9. Consequently, the use of a Gaussian mask requires an important number of filterings to reach the optimal fidelity F_{opt}. Indeed, in Fig. 9 the optimal fidelity is not yet reached after 40 filterings for low σ^2 values but for high σ^2 (i.e. *0.4 or 0.8 pixels*^{2}) F_{opt} is reached and has the same value that the one obtained with the mean mask of the same dimension.

Fig. 10 shows that for a Gaussian mask with a variance σ^2*=0.2 pixels*^{2}, the fidelity is independent of the mask dimension. Because the variance is low, elements located at the edges of the mask of dimension *n=5, 7, 9,...* have negligible irradiance. Hence their weight is negligible in the average realized during the filtering process. This is confirmed by Fig. 11 that shows the profiles of fringes filtered by Gaussian masks of dimension 3, 5, 7 and a variance σ^2*=0.2 pixels*^{2}. Hence, for σ^2*=0.2 pixels*^{2}, the only criterion for the choice of the mask dimension is the time spent to filter. As the duration of filtering decreases with the mask dimension, the dimension 3 is recommended for using the Gaussian filter.

Finally, it can be observed in Fig. 8 that the Gaussian filter induces a displacement of the phase steps. The latter is greater if the variance value is weak. This effect is due to the noise elimination: for a weak variance, noise is higher so it affects more significantly the average realized during the filtering process. The weight of noise in the average induces the slight displacement of the phase steps.

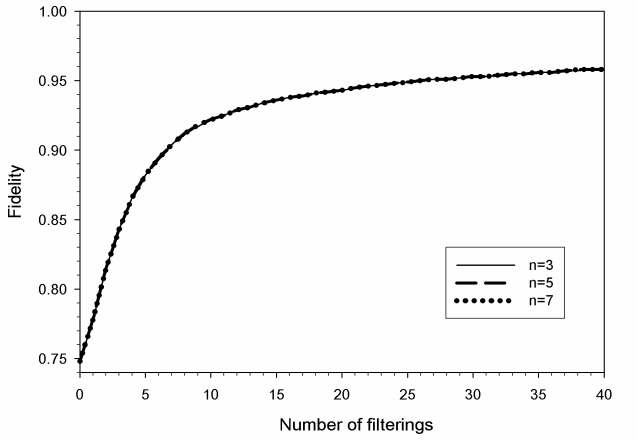

Fig. 10. Evolution of the fidelity versus the number of filterings for Gaussian masks of variance $\sigma^2=0.2\ pixels^2$, for dimensions n=3, 5 and 7: the fidelity curves are superimposed.

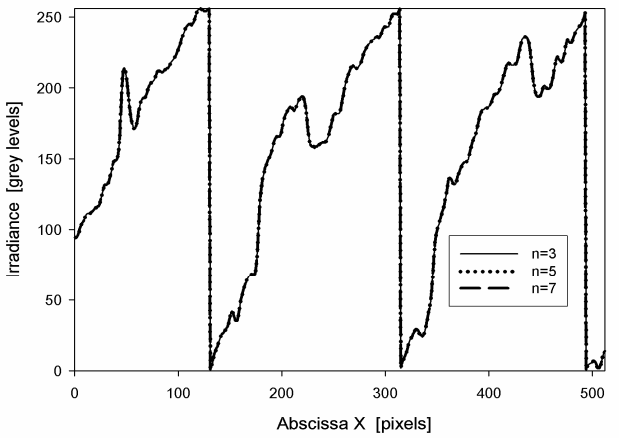

Fig. 11. Profiles of fringes filtered by Gaussian masks of variance $\sigma^2=0.2\ pixels^2$ and dimensions n=3, 5 and 7: the three profiles are superimposed.

3.3.3. Effect of the median mask

Fig. 12 shows the profiles of reference fringes and fringes filtered 40 times by a median mask of dimension 5. The median mask reduces noise more efficiently then the Gaussian mask but less then the mean mask. However, it is shown in Fig. 12 than the median mask preserves the slopes of rectangular signals better than the two masks studied previously. The correlation fringes filtered by the median mask have the higher contrast, as it is shown in Fig. 14. The high contrast obtained by the median mask is a significant advantage. Nevertheless, it appears that the median mask propagates the errors. Indeed, if an error covers an important number of pixels, then the filtering propagates it instead of its elimination, e.g. in Fig. 14.b the black fringes are rounded on the edges of the image and this effect grows with the number of applied filterings. Because of this parasitic effect, in practice, the number of filtering with the median mask must be limited (e.g. about 3 times).

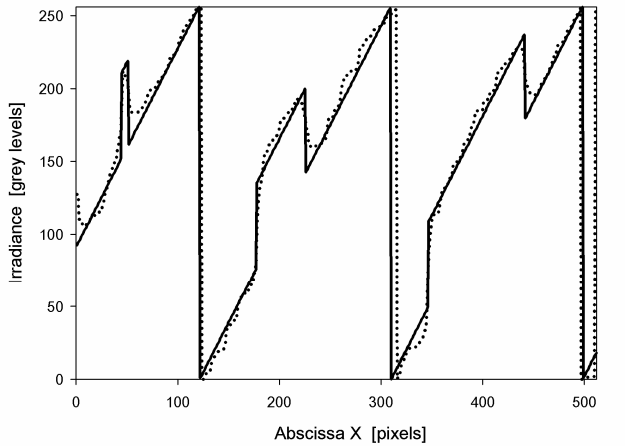

Fig. 12. Profile of the reference fringes (continuous line) and the ones filtered 40 times by a median mask of dimension 5 (dotted line).

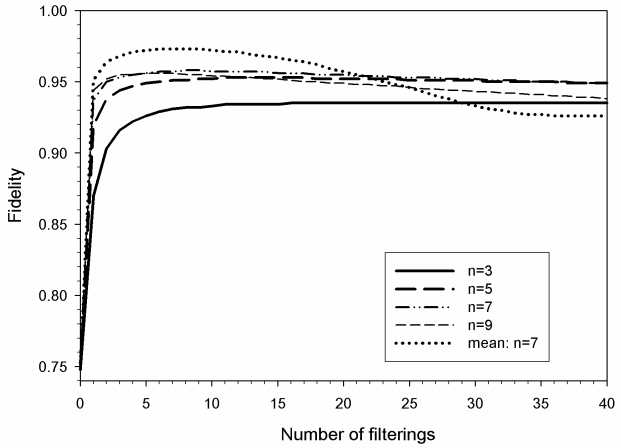

Fig. 13. Evolution of the fidelity versus the number of filterings for median masks of dimensions n=3, 5, 7, 9 and a mean mask of dimension n=7.

The fidelity versus the number of filterings and for different dimensions of the mask is presented in Fig. 13. Contrary to the mean and Gaussian masks, the optimal fidelity F_{opt} varies with the dimension of the median mask. It is shown in Fig. 13 that F_{opt} is higher for a median mask of dimension 7 then for median masks of dimensions 3, 5 or 9. Moreover the decrease of the fidelity, after having reached F_{opt}, is less significant for the median mask than for the mean mask. Indeed, after some filterings, the main effect of the median mask is the propagation of errors while the mean filter still averages the irradiance of the pixels.

Fig. 14 shows the reference fringes and the ones filtered the number of times corresponding to the optimal fidelity for each studied mask.

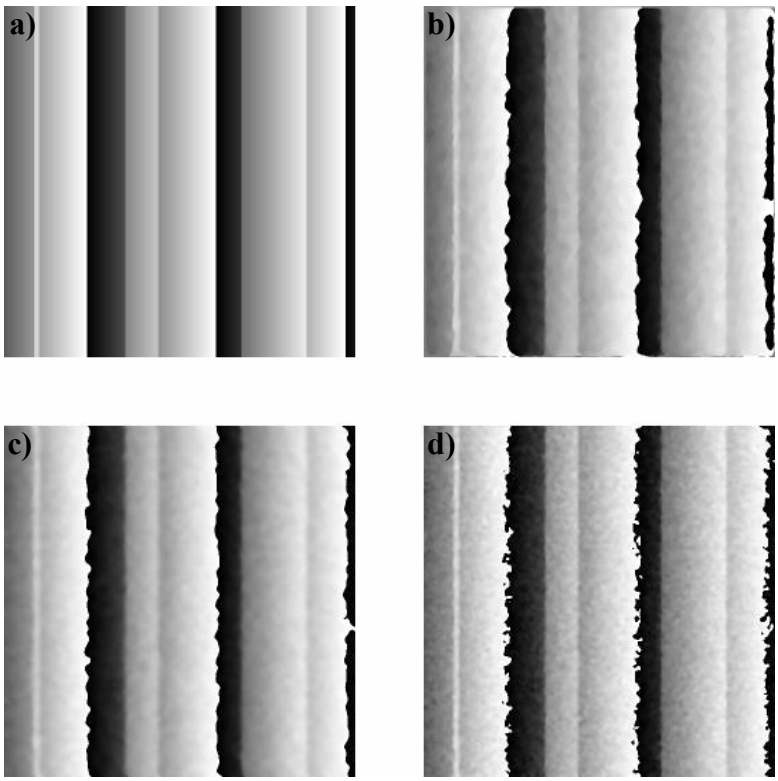

Fig. 14. a) Reference fringes. b) Correlation fringes filtered 7 times by a median mask of dimension 7. c) Fringes filtered 4 times by a mean mask of dimension 7. d) Fringes filtered 40 times by a Gaussian mask of dimension 5, $\sigma^2=0.2\ pixels^2$. The images are filtered the number of times corresponding to the optimal fidelity for each studied mask.

3.4. Experimental part

The three filtering masks studied previously (mean, Gaussian and median masks) have been tested by filtering an experimental wrapped phase map recorded in our laboratory thanks to an interferometric experimental setup of shearography[2, 6, 7] (or "Digital Shear Speckle Pattern Interferometry").

A set of 4 interference patterns, phase shifted the ones compared to the others, have been recorded in varying the voltage applied to the phase modulator, i.e. a liquid crystal variable retarder in our case. The latter was chosen because the interferometer is based on the separation of the polarization states TE (Transverse Electric) and TM (Transverse Magnetic). The shearographic experimental setup is shown in Fig. 15.

The light comes from a Nd-Yag laser diode (λ=532 nm). The object speckle pattern has been produced by retroscattering of the incident light on a steel plate (30 cm x 30 cm x 1 mm). The interferograms, more precisely the shearograms, recorded by a CMOS camera come from the interference between the object speckle wavefront and the same speckle wavefront shifted spatially along the X direction thanks to the shearing element. The latter is a coated prism (from "Edmund Optics") separating the two polarization modes thanks to the coating and a thin glass window glued on it.

We worked in an out-of-plane digital shearography arrangement (Fig. 15)[2, 6, 7]. The wrapped phase map has been obtained thanks to a four increments algorithm applied to the phase shifted recorded shearograms in two states of the steel plate: an initial state (steel plate at rest) and a loaded state (plate loaded centrally).

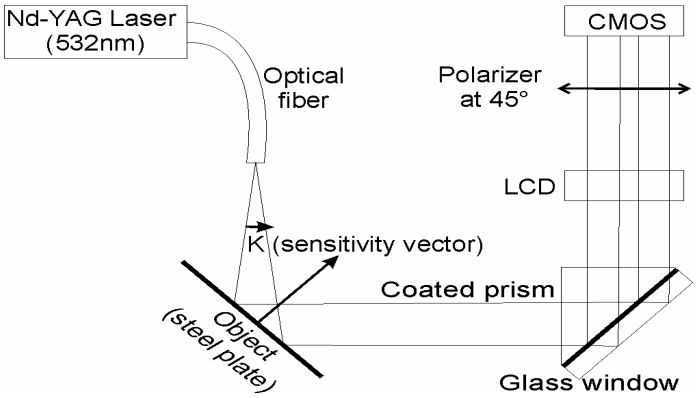

Fig. 15. Shearographic experimental setup for the recording of an experimental wrapped phase map.

Fig. 16.a shows an experimental shearogram recorded thanks to the setup presented in Fig. 15. This shearogram (Fig. 16.a) has been filtered by the different masks studied before: mean, Gaussian and median masks. As predicted by the section 3.3 , with regard to the elimination of noise, the mean filter is the most efficient (see Fig. 16.b) and the worse is the Gaussian mask. After a high number of filterings by a Gaussian mask, the experimental wrapped phase map looks like the one filtered just a few times by a mean mask. On the other hand, even if the median mask well preserves the contrast of fringes, after some filterings the errors on the edges of the image and other due to saturation of the pixels of the CMOS camera grow and make the filtered wrapped phase map difficult to manage for quantitative measurements.

In this study, it is thus the mean mask applied at the sine/cosine location in the filtering process (section 3.1) and just a few times (e.g. less than 5 times with a mask of maximum dimension 7) that yields the best results as well for removing noise and preserving the phase information as for the shortest filtering time. Fig. 16.b shows the shearogram from Fig. 16.a filtered 4 times by a mean mask of dimension 7 and Fig. 16.c, the corresponding profile. The masks studied in this work are elementary so they can be used easily and developed very quickly to filter data in laboratory. However, important improvement to filter data can be done by using more complex mask (e.g. anisotropic mask)[8] or transforms (e.g. Fourier or wavelet transform,…)[5, 9] and, in that case, the simple and systematic method developed in this work in order to evaluate the filters can be applied and appear useful.

4. CONCLUSION

In conclusion a simple and systematic method to study the behaviour of filters in order to use them in temporal phase shifting interferometry has been developed. The effects of elementary filters: mean, Gaussian and median masks, have been highlighted thanks to the analysis of profiles and fidelity functions between numerically synthesized reference fringes and the same ones disturbed by a Gaussian noise and next filtered by the studied filtering masks. On the other hand, the studied filters have been tested on an experimental wrapped phase map recorded in our laboratory. Finally, this study can be easily transposed to enhance the effects of more complex filters.

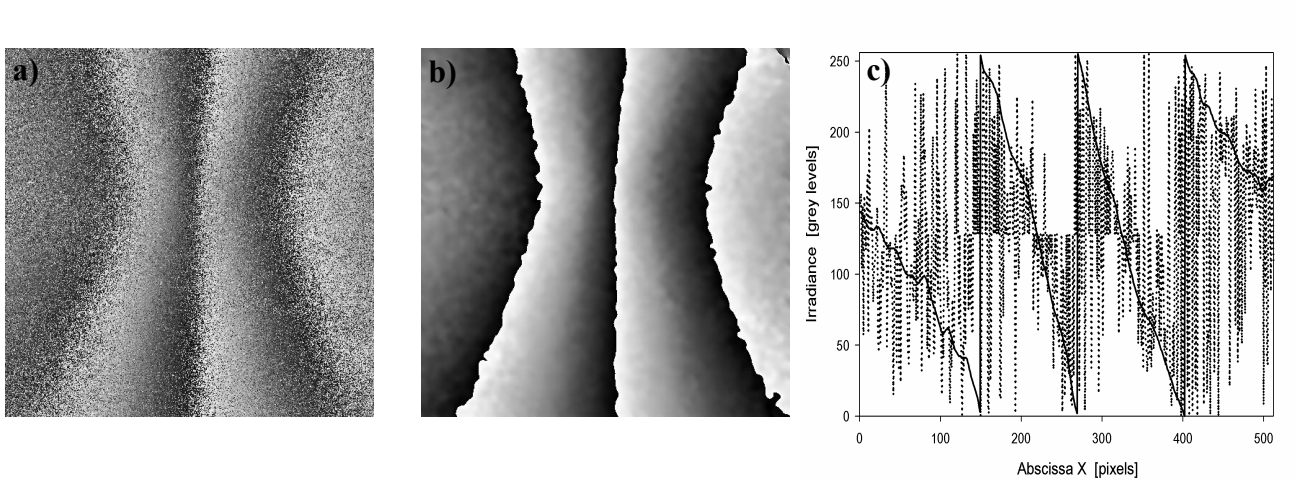

Fig. 16. a) Experimental shearogram recorded on the setup of Fig. 15. b) Shearogram of Fig.16.a filtered 4 times by a mean mask (section 3.3.1) of dimension 7. c) Profiles of the experimental fringes in Fig. 16.a (dotted line) and the ones filtered in Fig. 16.b (continuous line).

ACKNOWLEDGMENTS

Fabrice Michel, Ms Phys., is supported by a “First Entreprise” Project and Dr Vincent Moreau, by a “First Spin-Off” Project granted by the Research Dept. of the Walloon Region (Belgium).
Part of the work has been supported by a Cooperation Program Wallonie-Bruxelles/Quebec.
The authors also thank the ECA (European Center of Archeometry – University of Liège).

REFERENCES

1. P. K. Rastogi, *Digital Speckle Pattern Interferometry and Related Techniques* (John Wiley & Sons, Chichester, 2001).
2. W. Steinchen and L. Yang, *Digital Shearography* (SPIE Press, Bellingham, 2003).
3. Y. Renotte, D. Laboury, B. Tilkens, V. Moreau, and M. Morant, "At the crossing of Physics and Archeology : the OSIRIS Project (Optical Systems for Interferometric Relief Investigation and Scanning) - Development of a device for 3D numerical recording of archeological and epigraphic documents by optoelectronic processes," Europhysics News **35**(6), 205-207 (2004).
4. D. C. Ghiglia and M. D. Pritt, *Two-Dimensional Phase Unwrapping: Theory, Algorithms, and Software* (John Wiley & Sons, New York, 1998).
5. A. Federico and G. H. Kauffman, "Comparative study of wavelet tresholding methods for denoising electronic speckle pattern interferometry fringes," Optical Engineering **40**, 2598-2604 (2001).
6. V. M. Murukeshan, O. L. Seng, and A. Asundi, "Polarization phase shifting shearography for optical metrological applications," Optics & Laser Technology **30**(8), 527-531 (1998).
7. Y. Y. Hung, "Applications of digital shearography for testing of composite structures," Composites Part B: Engineering **30**(7), 765-773 (1999).
8. H. A. Aebischer and S. Waldner, "A simple and effective method for filtering speckle-interferometric phase fringe patterns," Optics Communications **162**(4-6), 205-210 (1999).
9. R. Kumar, S. Kumar Singh, and C. Shakher, "Wavelet filtering applied to time-average digital speckle pattern interferometry fringes," Optics & Laser Technology **33**(8), 567-571 (2001).